

Pump-seed synchronization for MHz repetition rate, high-power optical parametric chirped pulse amplification

Hanieh Fattahi,^{1,2,*} Catherine Yuriko Teisset,² Oleg Pronin,¹ Atsushi Sugita,¹
Roswitha Graf,^{1,2} Vladimir Pervak,² Xun Gu,¹ Thomas Metzger,^{1,2} Zsuzsanna Major,^{1,2}
Ferenc Krausz,^{1,2} and Alexander Apolonski^{1,2}

¹Max-Planck-Institut für Quantenoptik, Hans-Kopfermann-Str. 1, 85748 Garching, Germany

²Ludwig-Maximilians-Universität München (LMU), Am Coulombwall 1, 85748 Garching, Germany

*hanieh.fattahi@mpq.mpg.de

Abstract: We report on an active synchronization between two independent mode-locked lasers using a combined electronic-optical feedback. With this scheme, seed pulses at MHz repetition rate were amplified in a non-collinear optical parametric chirped pulse amplifier (OPCPA). The amplifier was seeded with stretched 1.5 nJ pulses from a femtosecond Ti:Sapphire oscillator, while pumped with the 1 ps, 2.9 μ J frequency-doubled output of an Yb:YAG thin-disk oscillator. The residual timing jitter between the two oscillators was suppressed to 120 fs (RMS), allowing for an efficient and broadband amplification at 11.5 MHz to a pulse energy of 700 nJ and an average power of 8 W. First compression experiment with 240 nJ amplified pulse energy resulted in a pulse duration of \sim 10 fs.

©2012 Optical Society of America

OCIS codes: (140.7090) Ultrafast lasers; (190.4410) Parametric processes; (320.7110) Ultrafast nonlinear optics; (190.4970) Parametric oscillators and amplifiers.

References and links

1. J. Lin, N. Weber, A. Wirth, S. H. Chew, M. Escher, M. Merkel, M. F. Kling, M. I. Stockman, F. Krausz, and U. Kleineberg, "Time of flight-photoemission electron microscope for ultrahigh spatiotemporal probing of nanoplasmonic optical fields," *J. Phys. Condens. Matter* **21**(31), 314005 (2009).
2. J. Ullrich, R. Moshhammer, A. Dorn, R. Dörner, L. P. H. Schmidt, and H. Schmidt-Böcking, "Recoil-ion and electron momentum spectroscopy: reaction-microscopes," *Rep. Prog. Phys.* **66**(9), 1463–1545 (2003).
3. S. Naumov, A. Fernandez, R. Graf, P. Dombi, F. Krausz, and A. Apolonski, "Approaching the microjoule frontier with femtosecond laser oscillators," *New J. Phys.* **7**, 216 (2005).
4. A. Dubietis, G. Jonusauskas, and A. Piskarskas, "Powerful femtosecond pulse generation by chirped and stretched pulse parametric amplification in BBO crystal," *Opt. Commun.* **88**(4-6), 437–440 (1992).
5. J. Neuhaus, D. Bauer, J. Zhang, A. Killi, J. Kleinbauer, M. Kumkar, S. Weiler, M. Guina, D. H. Sutter, and T. Dekorsy, "Subpicosecond thin-disk laser oscillator with pulse energies of up to 25.9 microjoules by use of an active multipass geometry," *Opt. Express* **16**(25), 20530–20539 (2008).
6. M. Schultze, T. Binhammer, G. Palmer, M. Emons, T. Lang, and U. Morgner, "Multi- μ J, CEP-stabilized, two-cycle pulses from an OPCPA system with up to 500 kHz repetition rate," *Opt. Express* **18**(26), 27291–27297 (2010).
7. M. Emons, A. Steinmann, T. Binhammer, G. Palmer, M. Schultze, and U. Morgner, "Sub-10-fs pulses from a MHz-NOPA with pulse energies of 0.4 μ J," *Opt. Express* **18**(2), 1191–1196 (2010).
8. C. Skrobol, I. Ahmad, S. Klingebiel, C. Wandt, S. A. Trushin, Z. Major, F. Krausz, and S. Karsch, "Broadband amplification by picosecond OPCPA in DKDP pumped at 515 nm," *Opt. Express* **20**(4), 4619–4629 (2012).
9. C. Y. Teisset, N. Ishii, T. Fuji, T. Metzger, S. Köhler, R. Holzwarth, A. Baltuška, A. M. Zheltikov, and F. Krausz, "Soliton-based pump-seed synchronization for few-cycle OPCPA," *Opt. Express* **13**(17), 6550–6557 (2005).
10. I. Ahmad, S. A. Trushin, Z. Major, C. Wandt, S. Klingebiel, T. J. Wang, V. Pervak, A. Popp, M. Siebold, F. Krausz, and S. Karsch, "Frontend light source for short-pulse pumped OPCPA system," *Appl. Phys. B* **97**(3), 529–536 (2009).
11. N. Ishii, L. Turi, V. S. Yakovlev, T. Fuji, F. Krausz, A. Baltuška, R. Butkus, G. Veitas, V. Smilgevičius, R. Danielius, and A. Piskarskas, "Multimillijoule chirped parametric amplification of few-cycle pulses," *Opt. Lett.* **30**(5), 567–569 (2005).

12. T. Binhammer, S. Rausch, M. Jackstadt, G. Palmer, and U. Morgner, "Phase-stable Ti:sapphire oscillator quasi-synchronously pumped by a thin-disk laser," *Appl. Phys. B* **100**(1), 219–223 (2010).
13. T. R. Schibli, J. Kim, O. Kuzucu, J. T. Gopinath, S. N. Tandon, G. S. Petrich, L. A. Kolodziejski, J. G. Fujimoto, E. P. Ippen, and F. X. Kaertner, "Attosecond active synchronization of passively mode-locked lasers by balanced cross correlation," *Opt. Lett.* **28**(11), 947–949 (2003).
14. S. V. Marchese, T. Südmeyer, M. Golling, R. Grange, and U. Keller, "Pulse energy scaling to 5 μ J from a femtosecond thin disk laser," *Opt. Lett.* **31**(18), 2728–2730 (2006).
15. V. Pervak, C. Y. Teisset, A. Sugita, S. Naumov, F. Krausz, and A. Apolonski, "High-dispersive mirrors for femtosecond lasers," *Opt. Express* **16**(14), 10220–10233 (2008).
16. T. Fuji, A. Unterhuber, V. S. Yakovlev, G. Tempea, A. Stingl, F. Krausz, and W. Drexler, "Generation of smooth, ultra-broadband spectra directly from a prism-less Ti:sapphire laser," *Appl. Phys. B* **77**(1), 125–128 (2003).
17. R. Paschotta, "Noise of mode-locked lasers (Part II): timing jitter and other fluctuations," *Appl. Phys. B* **79**(2), 163–173 (2004).
18. C. Hönninger, R. Paschotta, F. Morier-Genoud, M. Moser, and U. Keller, "Q-switching stability limits of continuous-wave passive mode locking," *J. Opt. Soc. Am. B* **16**(1), 46–56 (1999).
19. V. Pervak, I. Ahmad, M. K. Trubetskov, A. V. Tikhonravov, and F. Krausz, "Double-angle multilayer mirrors with smooth dispersion characteristics," *Opt. Express* **17**(10), 7943–7951 (2009).
20. I. T. Sorokina, "Cr²⁺-doped II–VI materials for lasers and nonlinear optics," *Opt. Mater.* **26**(4), 395–412 (2004).
21. W. Cao and Y. Duan, "Breath analysis: potential for clinical diagnosis and exposure assessment," *Clin. Chem.* **52**(5), 800–811 (2006).
22. O. Pronin, J. Brons, C. Grasse, V. Pervak, G. Boehm, M. C. Amann, V. L. Kalashnikov, A. Apolonski, and F. Krausz, "High-power 200 fs Kerr-lens mode-locked Yb:YAG thin-disk oscillator," *Opt. Lett.* **36**(24), 4746–4748 (2011).

1. Introduction

Ultrashort laser pulses with high average power at high repetition rates are highly demanded in many ultrafast experiments in order to decrease the measurement time and to increase the signal-to-noise ratio [1, 2]. Considering the scalability limitations of the Ti:Sapphire (Ti:Sa) technology in terms of pulse energy and repetition rate [3], optical parametric chirped pulse amplification (OPCPA) is a powerful alternative method for creating broadband few-cycle pulses [4]. The latest development of thin-disk oscillators resulted in 30 μ J, sub-ps, MW peak power pulses at MHz repetition rates [5] making them suitable for pumping OPCPAs. Short-pulse-pumped OPCPA allows the use of thinner amplifier crystals resulting in a large amplification bandwidth, while keeping the same gain level due to the higher possible pump intensity. 3 μ J pulses at 143 kHz have been demonstrated by using an optically synchronized regenerative amplifier and a Ti:Sa oscillator (two-laser approach) [6]. At a higher repetition rate of 1 MHz, sub-10 fs pulses with 420 nJ pulse energy and 0.4 W of average power have been shown [7]. In this one-laser approach a supercontinuum generated in bulk material provides the OPCPA seed. However, this scheme has the following drawbacks: i) the continuum is always centered at the wavelength of the pump laser and cannot be shifted to other spectral ranges and ii) it does not provide carrier-envelope-phase (CEP) stabilization. Therefore combining a Ti:Sa seed oscillator and an electronically synchronized pump oscillator would permit the generation of CEP-stabilized, few-cycle pulses at high repetition rates. Moreover, electronic synchronization between two independent mode-locked lasers is a universal approach and can be implemented for lasers operating in substantially different spectral ranges.

To maintain stable operation of the parametric amplifier and to avoid fluctuations of the amplified spectrum, pulse energy and pulse duration, the maximum timing jitter between the pump and seed sources needs to be less than 10% of the pump-pulse duration [8], imposing strict constraints on the pump-seed synchronization when picoseconds-scale pump pulses are used. In order to achieve this goal, several synchronization schemes have been reported. In passive synchronization [9–11], the OPCPA pump sources such as regenerative amplifiers or fiber lasers are seeded with the OPCPA seed oscillator. Synchronization can be achieved also by quasi-synchronously pumping of the seed oscillator [12]. Although in the above mentioned cases the pump and seed pulses are intrinsically synchronized, further synchronization of the seed and pump pulse trains at the OPCPA stage is required due to additional jitter introduced

by air turbulences, mechanical vibrations of optical components, temperature drifts and the finite stability of the frontend. In an active synchronization scheme, an electronic feedback loop controls the cavity length of one of the oscillators in order to control the timing jitter at the OPCPA stage. The feedback signal can be measured by electronic or optical detection. For the case of electronic detection the electronic phase measurement is done by comparing the repetition rates of two lasers, while the optical method uses a nonlinear interaction to measure directly the timing offset. Designing a control loop based on both electronic and an optical detection would allow the combination of the large dynamic range of electronic phase-locked loops (PLLs) with the timing precision of the optical detection. Using this principle, a jitter as low as 80 as has already been demonstrated for low-energy Ti:Sa and Cr:Forsterite oscillators [13]. Obviously such timing precision would be unnecessary for parametric amplifiers driven by 1-ps pump pulses. So far, active synchronization of lasers is mostly realized for mode-locked oscillators, with a typical output power of a few hundred milliwatt, which are intrinsically very stable. In this work, we developed a synchronization scheme combining an electronic loop based on a PLL and an optical control loop using balanced cross-correlation as the optical nonlinear interaction to synchronize a narrowband thin-disk oscillator with an average output power of tens of watts and a low-power Ti:Sa oscillator with 300 nm bandwidth. To our best knowledge, this is the first successful attempt of such type.

2. Mode-locked thin-disk oscillator

The pump source is based on an Yb:YAG thin-disk and long-cavity oscillator. The resonator, shown in Fig. 1, contains the Yb:YAG thin-disk (7%-doped, 200 μm -thick) used as a turning mirror. The thin-disk laser module from Dausinger & Giesen GmbH is pumped by fiber-coupled diodes at 940 nm wavelength. The pump spot diameter on the disk is 2.8 mm.

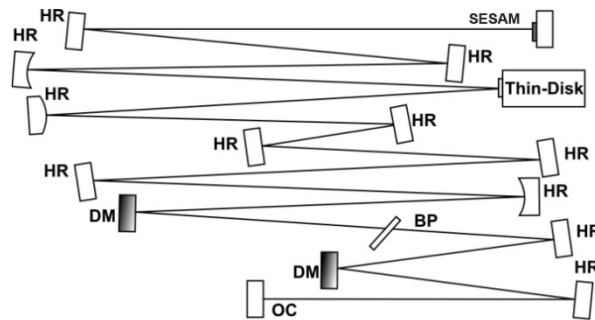


Fig. 1. Schematic of the Yb:YAG oscillator. HR, high reflector; DM, dispersive mirror; OC, output coupler; BP, Brewster plate; SESAM, Semiconductor Saturable Absorber Mirror.

A 1 mm thick fused silica Brewster plate is inserted to enforce linear polarisation. The oscillator is operating with a 12% output coupler. Passive mode-locking of the oscillator is achieved by using a commercially available Semiconductor Saturable Absorber Mirror (SESAM, BATOP, SAM-1040-1-500fs) as an end mirror of the cavity. The SESAM with a modulation depth of 0.5% is impinged by pulses with a peak intensity exceeding 4 GW/cm^2 . With a pump power of 260 W, 70 W of average power is obtained resulting in an optical-to-optical efficiency of 27%. In contrast to [14], the laser operates in air and delivers up to 6 μJ pulse energy at 11.5 MHz repetition rate with near-diffraction limited beam quality of $M^2 < 1.1$ (Fig. 2). Stable single-pulse operation was obtained with -18000 fs^2 of negative group delay dispersion (GDD) per round-trip. The dispersion was introduced by two highly dispersive mirrors [15] with -4500 fs^2 GDD per bounce. At 60 W output power, the oscillator exhibits a pulse duration of 1 ps and a bandwidth of 1.4 nm (FWHM) at a center wavelength of 1030 nm (Fig. 2). The RF-spectrum indicates strong sideband suppression above 60 dB (Fig. 2) around the repetition rate frequency.

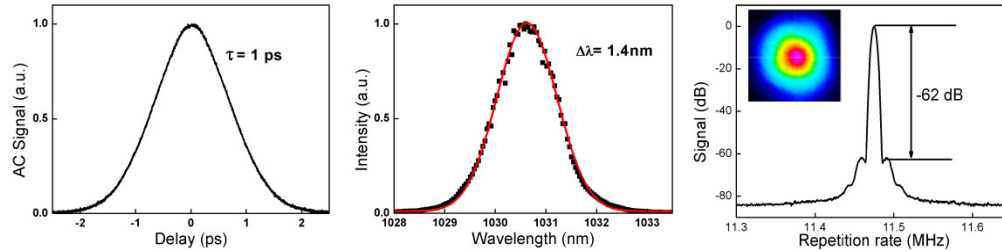


Fig. 2. The autocorrelation trace (left), optical spectrum (middle), the RF spectrum (right) and the beam profile (inset) of the Yb:YAG thin-disk oscillator.

3. Synchronization scheme

In order to synchronize the two independent lasers, we use an electronic synchronization with a feedback loop to correct the timing jitter. To increase the precision of the measured error signal, we developed a scheme combining an electronic and an optical control loop (Fig. 3) similar to that presented in [13].

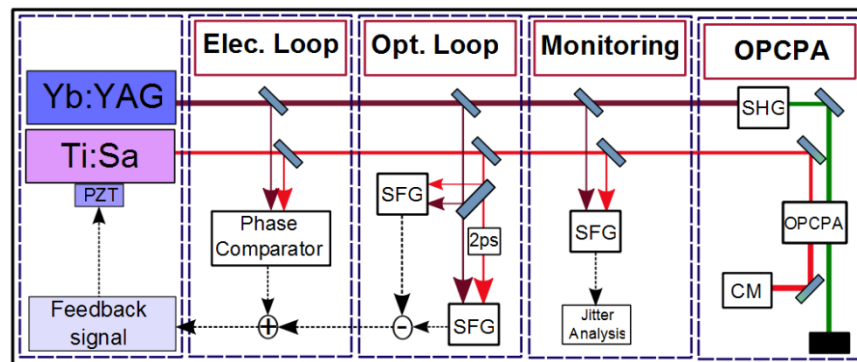


Fig. 3. Block diagram of the system; CM, chirped mirror.

In the system, the 7 fs Ti:Sa oscillator with 69 MHz repetition rate [16] is locked to the 11.5 MHz Yb:YAG laser. One of the folding mirrors in the Ti:Sa oscillator is mounted on a piezoelectric transducer (PZT). This configuration was chosen to avoid Q-switching instabilities in the Yb:YAG laser arising from sudden changes in the cavity. The PZT (PiezoJena P 25/10) has a response time of ms and a travel range of 50 μm . The locking proceeds in two steps. First, the electronic phase loop locks the pulse trains of the two oscillators. This is done by comparing the phase of the 36th harmonic of the repetition rate of the Yb:YAG and the 6th harmonic of the repetition rate of Ti:Sa oscillator at 414 MHz. The loop employs two standard 1-GHz-bandwidth photodiodes to detect the two pulse trains. After electronic locking, the sum frequency signal (SFG) of the optical loop can already be observed and traced (Fig. 4) although unstable at this point due to the high remaining timing jitter. In the second step, a balanced cross-correlator provides the feedback signal for the optical loop. As shown in Fig. 3, a fraction of the two laser pulses is directed onto two identical 2-mm thick BBO crystals for SFG. In one of the SFG setups, a 2 ps delay between the Ti:Sa and Yb:YAG pulses is introduced in order to determine the direction of the temporal offset. To produce the optical feedback signal, the two signals are recorded by two photodiodes and subtracted. When the temporal overlap between the two pulses at the position of the BBO crystals drifts, an asymmetric error signal is generated to readjust the position of the PZT (Fig. 5). This optical error signal adds a further correction to the electronic loop.

To investigate the locking performance of the synchronization, we set up a monitoring stage and measured the cross-correlation between the pulses of the lasers (Fig. 4). The timing jitter between the two lasers can be estimated from the width of the cross-correlation trace and the pulse durations of the two lasers. The monitoring stage (Fig. 3) consists of a 1-mm-thick BBO crystal and a photomultiplier for detecting the SFG. Assuming that the temporal shape of both laser pulses and the probability distribution of the timing jitter have a Gaussian distribution, the cross-correlation function is given by:

$$\tau_c = \sqrt{\tau_{\text{Ti:Sa}}^2 + \tau_{\text{Yb:YAG}}^2 + \tau_j^2} \quad (1)$$

where τ_j is the full width at half maximum (FWHM) of the timing jitter and τ_c is the FWHM of the cross-correlation. $\tau_{\text{Ti:Sa}}$ and $\tau_{\text{Yb:YAG}}$ are the pulse durations (FWHM) of the Ti:Sa and Yb:YAG oscillators, respectively. Due to the beam path in air and the transmission optics, the duration of the Ti:Sa pulses at the monitoring stage is elongated to 150 fs. From Eq. (1), the FWHM of the timing jitter between the two mode-locked oscillators can be estimated to an RMS value of 120 fs. For further characterization of the timing jitter, the pulse-to-pulse fluctuations of the SFG signal were analyzed at a delay of approximately half of the pump pulse duration. In this configuration, the timing jitter Δt is directly proportional to the measured intensity fluctuations ΔI (Fig. 6) and the RMS timing jitter σ_j can be retrieved from the RMS intensity fluctuations and the calibrated slope of the correlation curve. The coupling of intensity noise into timing noise has been thoroughly investigated in the case of passively mode-locked lasers [17]. To suppress the discrete nature of the pulse train at 11.5 MHz, a photomultiplier with a bandwidth below 500 kHz is used to measure the SFG. Figure 7 shows the recorded signal over 2 s. By calculating the Allan variance [17] of the recorded intensity noise, the frequency distribution of the timing jitter and thereby the time scale on which the timing jitter mostly occurs can be identified. From these data, the timing jitter is quantified in the range between 2 μs and 1 s as shown in Fig. 6. It can be seen that the main contribution of the timing jitter is located near 100 μs . The relaxation oscillation frequencies of the Ti:Sa and Yb:YAG lasers are estimated to be 140 kHz and 6.5 kHz, respectively [18]. The second value is very close to the highest component of the timing jitter located around 5 kHz. Therefore, it is most likely that the relaxation oscillations of the Yb:YAG are the main jitter source in our system.

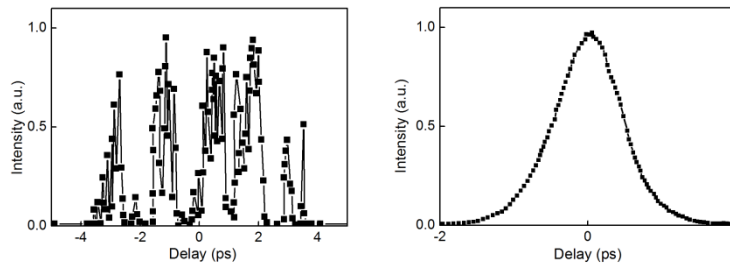


Fig. 4. The cross-correlation trace at the monitoring stage with only the electronic loop (left) and after activating the optical loop (right).

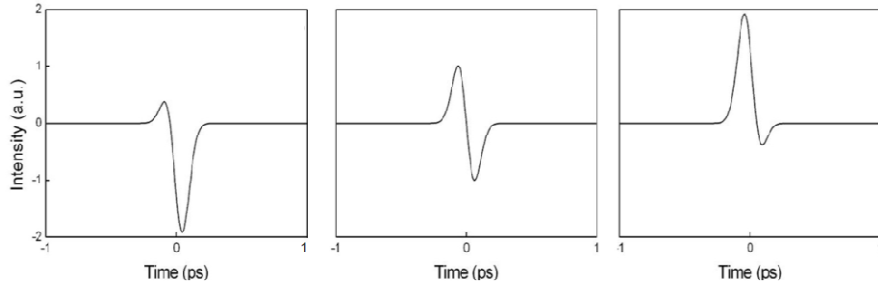


Fig. 5. Calculated error signal of the optical loop for -50 fs (left), 0 fs (middle) and $+50$ fs (right) timing offset between the two pulse trains.

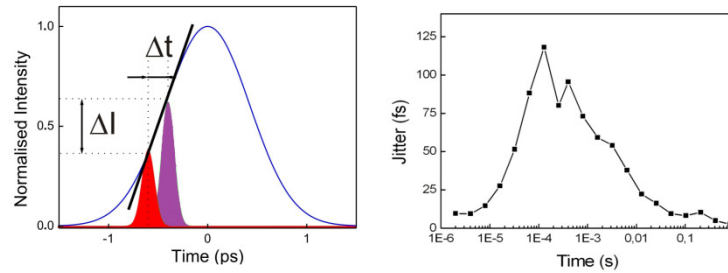


Fig. 6. Schematic representation of the timing jitter. Solid blue line, Yb:YAG pulse. Red and purple filled areas: SFG signal for different relative timing (left). The Allan variance of the measured timing jitter (right).

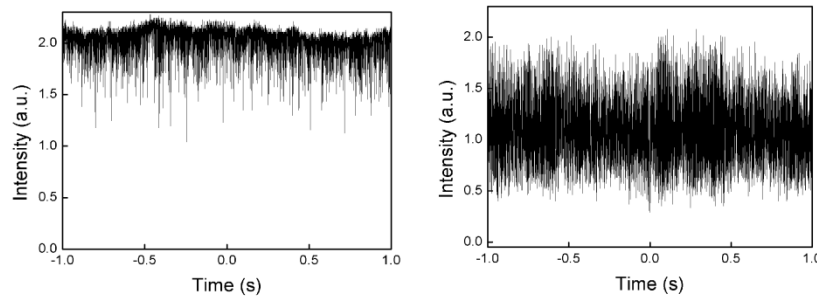


Fig. 7. The measured SFG at the monitoring stage: at the peak of the SFG signal (left), at the half of the SFG peak (right).

The quality of synchronization would certainly benefit from an optimization of the SESAM parameters and the cavity design to improve the stability performances of the oscillator. Another improvement of the timing jitter could be obtained by using a faster PZT thus increasing the feedback bandwidth of the active control loop. The residual jitter after the electronic and optical control loops is still within approximately 10% of the pump pulse width. These results allow for stable parametric amplification of the Ti:Sa seed pulses by using the frequency-doubled output of the Yb:YAG oscillator as a pump.

4. MHz OPCPA

The amplifier system consists of a single-stage non-collinear OPCPA and a chirped mirror compressor. To pump the parametric amplifier, the Yb:YAG pulses are frequency doubled in a 4 mm critically-phase-matched type-I LBO crystal, generating 43.5 W of 515 nm radiation with excellent beam quality. This corresponds to an optical efficiency of 65%. Due to strong saturation in the frequency conversion process, the pulse-to-pulse energy fluctuations at 515

nm are similar to that of the fundamental. The seed energy in front of the OPCPA crystal amounts to 1.4 nJ. The pump is focused to a beam diameter of 200 μm , slightly larger than the seed. Pump and seed are crossed at an internal angle $\alpha = 2.5^\circ$ inside a 4-mm BBO crystal cut at $\Theta = 24^\circ$ for type-I phase-matching. In this geometric configuration, the interaction length is longer than the crystal, ensuring good conversion efficiency and uniform amplification. Pumping the crystal with 34 W of average power and an intensity of 18 GW/cm^2 results in 5.6 W of amplified output power and a pump-to-signal conversion efficiency of 17% (Fig. 8). To improve the temporal overlap between pump and seed pulses, 16 mm uncoated fused silica was used to stretch the seed pulses to 500 fs resulting in 8 W of the amplified average power. This corresponds to a pulse energy of 700 nJ and a conversion efficiency of 24%. In this case, the amplified spectral bandwidth narrows, as shown in Fig. 8 but still supports a sub-7-fs Fourier-transform-limited pulse duration.

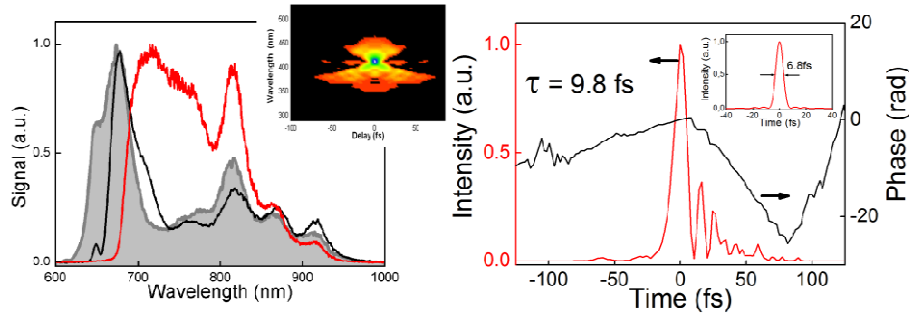


Fig. 8. Left: The seed spectrum (gray) and the amplified spectra at 490 nJ (black) and 700 nJ (red). Insert: retrieved FROG trace for 240 nJ. Right: FROG retrieval in the time domain. Insert: the transformed-limited pulse.

The superfluorescence background could not be measured with the power meter available to us. The superfluorescence ring was only visible by using a CCD camera and by removing the neutral density filter in front of it. The superfluorescence-to-signal ratio could be estimated to be on the order of 0.1%. On a time scale of 10 ms, the fluctuations of the amplified pulse train were similar to the fluctuations of the pump pulses. The preliminary compression was carried out by using a double-angle chirped-mirror compressor [19]. Since the only mirrors available to us had a relatively low GDD (-30 fs^2 per bounce), we minimised the introduced dispersion to the seed in order to reduce the amount of necessary bounces in the compressor. For this purpose the seed pulse duration was again decreased, by removing the stretcher and by using a thinner crystal in the OPCPA stage. Amplifying the seed in a 3 mm BBO crystal, we obtained 240 nJ pulse energy and a compressed pulse duration of 9.8 fs. The FROG trace (Fig. 8) shows satellite pulses which are caused by uncompensated higher-order dispersion. The quality of the compression can be improved further by using specially designed chirped mirrors.

5. Conclusion

In conclusion, we have realised a synchronization scheme with $< 120 \text{ fs}$ (RMS) timing jitter suitable for OPCPA systems pumped by a 1-ps laser source. Using this approach the 300 nm broadband spectrum of a Ti:Sa oscillator was amplified in a 4 mm BBO crystal to 700 nJ and 8 W of average power at 11.5 MHz repetition rate. 10 fs, 240 nJ pulses were realized with a 3 mm BBO crystal. Among others, this approach promises to reach CEP-stable μJ -level pulses at MHz repetition rate in the mid-infrared region [20], representing an attractive source e.g. for gas spectroscopy and gas analysis [21]. On the other hand, recent progress in generating even shorter pulses with high-power Yb-based oscillators [22] requires further improvement of the two-laser synchronization approach when short-pulse-pumped OPCPA is considered.

Acknowledgments

We acknowledge the technical support by L. Turi and S. Herbst. The work was supported by the Munich Centre for Advanced Photonics (MAP). Current address for C. Y. Teisset is: Coherent GmbH-Niederlassung Lübeck, Seeland str. 9, 23569 Lübeck, Germany. Current address for A. Sugita is: Department of Materials Science, Shizuoka University, 3-5-1 Johoku, Naka-ku, Hamamatsu 432-8561, Japan.